International Journal of Pure and Applied Mathematics

Volume 13 No. 3 2004, 391-411

EFFICIENT NUMERICAL SOLUTION OF 3D INCOMPRESSIBLE VISCOUS NAVIER-STOKES EQUATIONS

Salwa K. Abd-El-Hafiz[1] §, Gamal A.F. Ismail[2], Berlant S. Matit[3]

[1]Engineering Mathematics Department
Faculty of Engineering
Cairo University
Giza 12211, EGYPT
e-mail: salwahafiz@link.net

[2,3]Department of Applied Mathematics
Women's College
Ain Shams University
Cairo, EGYPT

Abstract: This paper focuses on the numerical solution of the three dimensional incompressible viscous Navier-Stokes equations. Using the vorticity-vector potential approach, a technique for the solution of the Navier-Stokes equations is presented. The parabolic vorticity transport equation and the elliptic Poisson equation are discretized in a collocated Cartesian grid. Using the finite difference method, an iterative technique for the solution of the three dimensional Poisson equation is presented. With respect to the vorticity transport equation, the explicit Euler method is used. In addition, we study the boundary conditions as well as the stability of the numerical techniques. Finally, we present our time-marching algorithm. The correctness of the algorithm is demonstrated on the model problem of the lid-driven cavity in three-dimensional space.

AMS Subject Classification: 35Q30, 65M06, 65M12
Key Words: finite difference, elliptic Poisson equation, parabolic vorticity transport equation, lid-driven cavity

Received: March 28, 2004

§Correspondence author

1. Introduction

The solution of Navier-Stokes equations is, in general, essential for the characterization and understanding of several problems involving phenomena and/or industrial processes such as supersonic flows, fluid motions in electrolytic reduction cells and electromagnetic stirring [2, 7, 18, 23]. In the past, numerous efforts involved a lot of simplifying assumptions that were necessary to make the problems tractable. Moreover, obtaining those analytical solutions was only possible for linear problems restricted to one or two dimensional simple geometries [14]. It was, thus, obvious to turn to numerical techniques as a mean for taking such problems in a realistic manner.

The efficient solution of the Navier-Stokes equations is still one of the challenging numerical tasks, especially in three dimensional space (3D). The most popular and most thoroughly studied methods for treating problems of this type are based on finite difference discretizations (see, for example, [21]). Section 2 of this paper presents the Navier-Stokes continuity and momentum equations and briefly reviews related literature. Section 3 derives the 3D vorticity-vector potential approach. In Section 4, we discuss four basic subjects related to the design of finite difference methods for 3D steady incompressible viscous flows using vorticity formulations: boundary conditions, Poisson equation, vorticity transport equation and a time-marching algorithm. In Section 5, the time-marching algorithm is applied on the model problem of the lid-driven cavity in 3D. Finally, concluding remarks and directions for future research are outlined in Section 6.

2. Navier-Stokes Equations

The conservation of mass law applied to a fluid passing through an infinitesimal, fixed control volume yields the following equation of continuity

$$\frac{\partial \rho}{\partial t} + \bigtriangledown \cdot (\rho V) = 0, \tag{1}$$

where, ρ is the fluid density and V is the fluid velocity. It is convenient to use the substantial derivative

$$\frac{D(..)}{Dt} \equiv \frac{\partial(..)}{\partial t} + V \cdot \bigtriangledown(..), \tag{2}$$

to change equation (1) into the form:

$$\frac{D\rho}{Dt} + \rho(\nabla \cdot V) = 0. \tag{3}$$

We will adopt the definition that incompressible flow is the same as constant density flow. Given this definition, the continuity equation becomes:

$$\nabla \cdot V = 0. \tag{4}$$

The momentum equation is deduced by applying Newton Second Law to a fluid passing through an infinitesimal, fixed control volume. Assuming that the flow is incompressible and that the coefficient of viscosity is constant, the momentum equation can be written as:

$$\rho \frac{DV}{Dt} = \rho F - \nabla p + \mu \nabla^2 V, \tag{5}$$

where, p is the pressure, F is a given externally applied force and μ is the coefficient of viscosity. The above equation may also be written as:

$$\frac{DV}{Dt} = F - \frac{1}{\rho} \nabla p + \nu \nabla^2 V, \tag{6}$$

where, ν is the kinematic viscosity.

The mathematical formulations that are commonly used to simulate 3D incompressible viscous flows include the primitive-variables (velocity-pressure), and vorticity-vector potential formulations. Each formulation has its own advantages with respect to the other.

The vorticity-vector potential approach has a distinct advantage over the velocity-pressure formulation in that the pressure need not be calculated explicitly. Examples of this approach can be found in [14, 19]. Its importance is explained by Aziz and Hellums [3] and some recent advances are illustrated by Weinan [21, 22].

The primitive-variables approach is receiving increased attention because it is applicable to transient problems in 3D. Some of the important studies in this approach are essentially due to Chorin [5, 6]. Chorin developed the artificial compressibility method for handling viscous incompressible flows. A successful implicit formulation in terms of primitive-variables was also developed by Patanker and Spalding [16]. These implicit methods have an advantage over the explicit algorithms in that they have no restrictions on the time step from the point of view of numerical stability (see, for example, [8, 15, 20]).

Pujol [17] used Chorin method and compared it to a stream function-vorticity approach for a two-dimensional viscous problem. He concluded that the stream function-vorticity approach is preferable because we only consider velocity boundary conditions. This is usually simpler than considering both velocity and pressure boundary conditions.

3. Vorticity-Vector Potential Approach

For a Cartesian coordinate system, where u, v, w represent the x, y, z components of the velocity vector, the continutiy and momentum equations become:

$$\text{continuity equation:} \quad \frac{\partial u}{\partial x} + \frac{\partial v}{\partial y} + \frac{\partial w}{\partial z} = 0, \tag{7}$$

$$x\text{-momentum:} \ \rho\frac{\partial u}{\partial t} + \rho u\frac{\partial u}{\partial x} + \rho v\frac{\partial u}{\partial y} + \rho w\frac{\partial u}{\partial z} = -\frac{\partial p}{\partial x} + \rho f_x + \mu\nabla^2 u, \tag{8}$$

$$y\text{-momentum:} \ \rho\frac{\partial v}{\partial t} + \rho u\frac{\partial v}{\partial x} + \rho v\frac{\partial v}{\partial y} + \rho w\frac{\partial v}{\partial z} = -\frac{\partial p}{\partial y} + \rho f_y + \mu\nabla^2 v, \tag{9}$$

$$z\text{-momentum:} \ \rho\frac{\partial w}{\partial t} + \rho u\frac{\partial w}{\partial x} + \rho v\frac{\partial w}{\partial y} + \rho w\frac{\partial w}{\partial z} = -\frac{\partial p}{\partial z} + \rho f_z + \mu\nabla^2 w. \tag{10}$$

The vector potential ψ is defined as

$$V = \nabla \times \psi. \tag{11}$$

The vorticity ξ is defined as

$$\xi = \nabla \times V. \tag{12}$$

Inserting equation (11) into equation (12) we obtain

$$\nabla \times (\nabla \times \psi) = \xi, \tag{13}$$

or

$$\nabla(\nabla \cdot \psi) - \nabla^2\psi = \xi.$$

We can choose ψ to satisfy

$$\nabla \cdot \psi = 0. \tag{14}$$

So, equation (13) becomes

$$\nabla^2\psi = -\xi. \tag{15}$$

This vector Poisson equation represents three scalar Poisson equations, which must be solved after each time step.

In addition, by differentiating the momentum equations and using the continuity equation, the momentum equations can be reduced to the three scalar parabolic equations:

$$x\text{-momentum:} \quad \frac{D\xi_x}{Dt} = \xi_x\frac{\partial u}{\partial x} + \xi_y\frac{\partial u}{\partial y} + \xi_z\frac{\partial u}{\partial z} + \nu\nabla^2\xi_x + \frac{\partial f_y}{\partial z} - \frac{\partial f_z}{\partial y}, \tag{16}$$

$$y\text{-momentum:} \quad \frac{D\xi_y}{Dt} = \xi_x\frac{\partial v}{\partial x} + \xi_y\frac{\partial v}{\partial y} + \xi_z\frac{\partial v}{\partial z} + \nu\nabla^2\xi_y + \frac{\partial f_z}{\partial x} - \frac{\partial f_x}{\partial z}, \quad (17)$$

$$z\text{-momentum:} \quad \frac{D\xi_z}{Dt} = \xi_x\frac{\partial w}{\partial x} + \xi_y\frac{\partial w}{\partial y} + \xi_z\frac{\partial w}{\partial z} + \nu\nabla^2\xi_z + \frac{\partial f_x}{\partial y} - \frac{\partial f_y}{\partial x}. \quad (18)$$

Thus, the vector vorticity transport equation in 3D is written as:

$$\frac{D\xi}{Dt} = (\xi \cdot \bigtriangledown)V + \nu\nabla^2\xi + \nabla \times F, \quad (19)$$

where we assume that the partial derivatives $\frac{\partial f_y}{\partial z}$, $\frac{\partial f_z}{\partial y}$, $\frac{\partial f_z}{\partial x}$, $\frac{\partial f_x}{\partial z}$, $\frac{\partial f_x}{\partial y}$ and $\frac{\partial f_y}{\partial x}$ are continuous. The equation is applied three times for the three different directions x, y and z. Hence, we will solve three parabolic and three elliptic PDE at each time level.

4. Numerical Implementation of the Vorticity-Vector Potential Approach

In this section, we discuss four basic topics related to the design of finite difference methods for 3D steady incompressible viscous flows using vorticity formulations. These topics are the boundary conditions, Poisson equation, vorticity transport equation and its stability and the time-marching algorithm.

Boundary Conditions. The boundary conditions for the incompressible Navier-Stokes equations commonly consist of specifying a value for the unknown (Dirichlet) or specifying a value for its gradient normal to the boundary (Neumann). These conditions follow directly from the physical nature of the boundaries, e.g., solid boundaries or walls.

In case of 3D incompressible Navier-Stokes equations in a closed domain, the velocity normal to the boundary is zero. For instance, on the plane x =constant the velocity component u is zero. From the definition of ψ, it follows that $u = \frac{\partial \psi_z}{\partial y} - \frac{\partial \psi_y}{\partial z} = 0$. This implies that the potential components ψ_z and ψ_y may be taken as constants. Thus, we arbitrarily choose ψ_z and ψ_y to be zero. Due to the solenoidal property of ψ ($\nabla \cdot \psi = 0$), it then follows that $\frac{\partial \psi_x}{\partial x} = 0$. Hence, on the wall x =constant, the conditions on ψ are:

$$\frac{\partial \psi_x}{\partial x} = \psi_y = \psi_z = 0 \quad \text{on} \quad x = \text{constant}, \quad (20)$$

On the other hand, the no-slip condition implies that at the plane x =constant, for example, we have

$$\frac{\partial v_i}{\partial y} = 0, \quad \frac{\partial v_i}{\partial z} = 0\,, \quad \forall i = 1, 2, 3\,, \tag{21}$$

where, v_i are the components of the velocity V. Thus, the vorticity boundary conditions can be expressed in terms of the vector potential components. For instance, the vorticity boundary conditions for a wall x =constant are:

$$\xi_y = -\frac{\partial w}{\partial x} = -\frac{\partial}{\partial x}\left(\frac{\partial \psi_y}{\partial x} - \frac{\partial \psi_z}{\partial y}\right) = -\frac{\partial^2 \psi_y}{\partial x^2} + \frac{\partial}{\partial y}\left(\frac{\partial \psi_z}{\partial x}\right). \tag{22}$$

From equation (20), the previous equation becomes

$$\xi_y = -\frac{\partial^2 \psi_y}{\partial x^2}. \tag{23}$$

In a similar manner, we can show that

$$\xi_z = -\frac{\partial^2 \psi_z}{\partial x^2}. \tag{24}$$

Then, we can write:

$$\xi_x = 0,\ \xi_y = -\frac{\partial^2 \psi_y}{\partial x^2},\ \xi_z = -\frac{\partial^2 \psi_z}{\partial x^2} \quad \text{on} \quad x = \text{constant}. \tag{25}$$

Using a second-order centered difference approximation for the second derivative, equation (23) at (x_0, y_j, z_k) becomes

$$\xi_y(x_0, y_j, z_k) = -\frac{1}{(\triangle x)^2}\left[\psi_y(x_1, y_j, z_k) - 2\psi_y(x_0, y_j, z_k) + \psi_y(x_{-1}, y_j, z_k)\right]. \tag{26}$$

Using equation (20), we get

$$\xi_y(x_0, y_j, z_k) = -\frac{1}{(\triangle x)^2}\left[\psi_y(x_1, y_j, z_k) + \psi_y(x_{-1}, y_j, z_k)\right]. \tag{27}$$

From equation (11) we have

$$w(x_0, y_j, z_k) = \frac{\partial \psi_y}{\partial x}|_{0,j,k} - \frac{\partial \psi_x}{\partial y}|_{0,j,k}. \tag{28}$$

If we use a second-order centered difference approximation for the first derivatives and rearrange the above equation, we get

$$\psi_y(x_{-1}, y_j, z_k) = \psi_y(x_1, y_j, z_k) - 2\triangle x \left[\frac{\partial \psi_x}{\partial y}|_{0,j,k} + w(x_0, y_j, z_k) \right]. \quad (29)$$

So, equation (27) becomes

$$\xi_y(x_0, y_j, z_k) = -\frac{2}{(\triangle x)^2}\psi_y(x_1, y_j, z_k) + \frac{2}{\triangle x}\left[\frac{\partial \psi_x}{\partial y}|_{0,j,k} + w(x_0, y_j, z_k) \right]. \quad (30)$$

In the same way we will find

$$\xi_z(x_0, y_j, z_k) = -\frac{2}{(\triangle x)^2}\psi_z(x_1, y_j, z_k) + \frac{2}{\triangle x}\left[\frac{\partial \psi_x}{\partial z}|_{0,j,k} + v(x_0, y_j, z_k) \right]. \quad (31)$$

It should be pointed out that there are different alternatives for expressing the boundary conditions. Some approaches obtain the vorticity (ξ) at the boundary in terms of the velocity [3, 8, 18]. These methods have a first-order accuracy. To improve the accuracy, we have obtained (ξ) at the boundary in terms of (ψ) [22]. Thus, our method has a second-order accuracy.

Poisson Equation. For the domain $D = [0, a] \times [0, b] \times [0, c] \in R^3$, we use a grid with n cells in the x-direction, q cells in the y-direction and s cells in the z-direction of equal sizes. The distance between two grid points can be computed by:

$$\triangle x = \frac{a}{n}, \quad \triangle y = \frac{b}{q}, \quad \triangle z = \frac{c}{s}.$$

Thus, a finite difference formulation for Poission equation (15) is as follows:

$$\frac{\psi^m_{i+1,j,k} - 2\psi^m_{i,j,k} + \psi^m_{i-1,j,k}}{(\triangle x)^2} + \frac{\psi^m_{i,j+1,k} - 2\psi^m_{i,j,k} + \psi^m_{i,j-1,k}}{(\triangle y)^2} + \frac{\psi^m_{i,j,k+1} - 2\psi^m_{i,j,k} + \psi^m_{i,j,k-1}}{(\triangle z)^2} = -\xi^m_{i,j,k}, \quad (32)$$

This implies that:

$$\begin{aligned} &2\psi_{i,j,k}[(\triangle x)^2(\triangle z)^2 + (\triangle x)^2(\triangle y)^2 + (\triangle y)^2(\triangle z)^2] \\ &\quad - (\triangle y)^2(\triangle z)^2[\psi_{i+1,j,k} + \psi_{i-1,j,k}] - (\triangle x)^2(\triangle y)^2[\psi_{i,j,k+1} + \psi_{i,j,k-1}] \\ &\quad\quad - (\triangle x)^2(\triangle z)^2[\psi_{i,j+1,k} + \psi_{i,j-1,k}] = (\triangle x)^2(\triangle y)^2(\triangle z)^2\xi_{i,j,k}, \quad (33) \end{aligned}$$

for each $i = 1, 2, \ldots, n-1$, $j = 1, 2, \ldots, q-1$ and $k = 1, 2, \ldots, s-1$. Note that no time index is specified in equation (33) because all variables are given at the same time. In addition, the equation is applied three times for the three different directions x, y and z.

There are two techniques for the solution: a direct method and an iterative method. In the direct method, a linear system of equations is formed. This system could, in principal, be solved for $\psi_{i,j,k}$ for all points in the interior of the domain D. This is a difficult set of equations to solve because the number of unknowns can be very large. For example, a lattice with 100 points in each of x, y and z directions, has 10^6 points.

On the other hand, iterative methods are ideal for solving this 3D Poisson equation. Examples of these techniques are found in [4, 10]. To illustrate such techniques, rewrite Poisson equation as:

$$\begin{aligned}\psi_{i,j,k}^{(p+1)} = {} & \frac{1}{2[(\triangle x)^2(\triangle z)^2 + (\triangle x)^2(\triangle y)^2 + (\triangle y)^2(\triangle z)^2]} \\ & \times \{(\triangle y)^2(\triangle z)^2[\psi_{i+1,j,k}^{(p)} + \psi_{i-1,j,k}^{(p)}] + (\triangle x)^2(\triangle y)^2[\psi_{i,j,k+1}^{(p)} + \psi_{i,j,k-1}^{(p)}] \\ & + (\triangle x)^2(\triangle z)^2[\psi_{i,j+1,k}^{(p)} + \psi_{i,j-1,k}^{(p)}] + (\triangle x)^2(\triangle y)^2(\triangle z)^2\xi_{i,j,k}^{(p)}\}, \quad (34)\end{aligned}$$

where, the superscript p ($p \geq 0$) refers to the iteration number. The algorithm is primed with an initial guess $\psi_{i,j,k}^{(0)}$ for all values of i, j and k and the solution is iterated until convergence. The condition of convergence is:

$$\max_{i,j,k} |\psi_{i,j,k}^{(p+1)} - \psi_{i,j,k}^{(p)}| \leq \epsilon, \quad (35)$$

where ϵ is a small pre-defined positive value.

The iterative numerical solution is unconditionally stable, i.e. it will always converge to a solution. The accuracy of the solution depends on the adequacy of the numerical grid to describe the regions of high curvature of the vector potential and on the ability of the numerical grid to cover the domain [9].

Vorticity Transport Equation. To obtain a numerical solution of equation (19), we can apply two methods: Euler explicit method and Crank-Nicolson (C-N) implicit method [13, 18]. The explicit method enables the computation of ξ at a single grid point of the advanced time-level $(m+1)$ in terms of the values at the previous time level (m). This process is often referred as "time-marching". This method does not demand the solution of a linear system of equations at each time step; its implementation is therefore very fast. Of course, there are restrictions on the time step size in order to have a stable solution.

In the implicit method, we must evaluate all values of ξ at time level $(m+1)$ in terms of those at time-level (m). This is carried out by solving a linear system of equations at each time step. Therefore, the computation time is more in the implicit method than in the explicit method. The computation time difference is not significant for 1D problems. For 2D and 3D problems, however, we have to solve large systems of equations for each advance in time. Thus, the size of the computer memory limits the ability of performing reasonable spatial discretizations. Implicit methods, on the other hand, have improved stability properties [7]. With respect to truncation errors, Euler method is second-order in space and first-order in time, whereas C-N method is second-order in space and time [7].

In 3D Navier-Stokes equations, Euler explicit method is preferred because it does not limit the spatial discretizations [21, 22]. In this method, we replace the time derivatives in equation (19) with forward differences. The spatial first-order and second-order derivatives are replaced with second-order central differences. Therefore, equation (16) can be written as:

$$\begin{aligned}
(\xi_x)^{m+1}_{i,j,k} = (\xi_x)^m_{i,j,k} &- (u)^m_{i,j,k}\ \frac{\triangle t}{2\triangle x}\left[(\xi_x)^m_{i+1,j,k} - (\xi_x)^m_{i-1,j,k}\right] \\
&- (v)^m_{i,j,k}\ \frac{\triangle t}{2\triangle y}\left[(\xi_x)^m_{i,j+1,k} - (\xi_x)^m_{i,j-1,k}\right] \\
&- (w)^m_{i,j,k}\ \frac{\triangle t}{2\triangle z}\left[(\xi_x)^m_{i,j,k+1} - (\xi_x)^m_{i,j,k-1}\right] \\
&+ (\xi_x)^m_{i,j,k}\ \frac{\triangle t}{2\triangle x}\left[(u)^m_{i+1,j,k} - (u)^m_{i-1,j,k}\right] \\
&+ (\xi_y)^m_{i,j,k}\ \frac{\triangle t}{2\triangle y}\left[(u)^m_{i,j+1,k} - (u)^m_{i,j-1,k}\right] \\
&+ (\xi_z)^m_{i,j,k}\ \frac{\triangle t}{2\triangle z}\left[(u)^m_{i,j,k+1} - (u)^m_{i,j,k-1}\right] \\
&+ \nu\ \frac{\triangle t}{(\triangle x)^2}\left[(\xi_x)^m_{i+1,j,k} - 2(\xi_x)^m_{i,j,k} + (\xi_x)^m_{i-1,j,k}\right] \\
&+ \nu\ \frac{\triangle t}{(\triangle y)^2}\left[(\xi_x)^m_{i,j+1,k} - 2(\xi_x)^m_{i,j,k} + (\xi_x)^m_{i,j-1,k}\right] \\
&+ \nu\ \frac{\triangle t}{(\triangle z)^2}\left[(\xi_x)^m_{i,j,k+1} - 2(\xi_x)^m_{i,j,k} + (\xi_x)^m_{i,j,k-1}\right] \\
&+ \triangle t\left[\frac{(f_z)^m_{i,j+1,k} - (f_z)^m_{i,j-1,k}}{2\triangle y} - \frac{(f_y)^m_{i,j,k+1} - (f_y)^m_{i,j,k-1}}{2\triangle z}\right], \quad (36)
\end{aligned}$$

where, m denotes the time level.

The other two momentum equations for obtaining ξ_y and ξ_z can be analyzed in an analogous manner. Because the time t can vary in an unbounded range $0 \leq t \leq \infty$, it is important to study the possible instability of the method. Let us study the stability of equation (36), which is rewritten as:

$$(\xi_x)^{m+1}_{i,j,k} = G(\xi_x)^m_{i,j,k} + \triangle t H(x_i, y_j, z_k), \tag{37}$$

where

$$\begin{aligned} H(x_i, y_j, z_k) = (\xi_y)^m_{i,j,k} \, \frac{1}{2\triangle y} \left[(u)^m_{i,j+1,k} - (u)^m_{i,j-1,k}\right] \\ + (\xi_z)^m_{i,j,k} \, \frac{1}{2\triangle z} \left[(u)^m_{i,j,k+1} - (u)^m_{i,j,k-1}\right] \\ + \frac{1}{2\triangle z} \left[(f_y)^m_{i,j,k+1} - (f_y)^m_{i,j,k-1}\right] - \frac{1}{2\triangle y} \left[(f_z)^m_{i,j+1,k} - (f_z)^m_{i,j-1,k}\right]. \end{aligned} \tag{38}$$

and

$$\begin{aligned} G(\xi_x)^m_{i,j,k} = (\xi_x)^m_{i,j,k} - (u)^m_{i,j,k} \, \frac{\triangle t}{2\triangle x} \left[(\xi_x)^m_{i+1,j,k} - (\xi_x)^m_{i-1,j,k}\right] \\ - (v)^m_{i,j,k} \, \frac{\triangle t}{2\triangle y} \left[(\xi_x)^m_{i,j+1,k} - (\xi_x)^m_{i,j-1,k}\right] \\ - (w)^m_{i,j,k} \, \frac{\triangle t}{2\triangle z} \left[(\xi_x)^m_{i,j,k+1} - (\xi_x)^m_{i,j,k-1}\right] \\ + (\xi_x)^m_{i,j,k} \, \frac{\triangle t}{2\triangle x} \left[(u)^m_{i+1,j,k} - (u)^m_{i-1,j,k}\right] \\ + \nu \, \frac{\triangle t}{(\triangle x)^2} \left[(\xi_x)^m_{i+1,j,k} - 2(\xi_x)^m_{i,j,k} + (\xi_x)^m_{i-1,j,k}\right] \\ + \nu \, \frac{\triangle t}{(\triangle y)^2} \left[(\xi_x)^m_{i,j+1,k} - 2(\xi_x)^m_{i,j,k} + (\xi_x)^m_{i,j-1,k}\right] \\ + \nu \, \frac{\triangle t}{(\triangle z)^2} \left[(\xi_x)^m_{i,j,k+1} - 2(\xi_x)^m_{i,j,k} + (\xi_x)^m_{i,j,k-1}\right]. \end{aligned} \tag{39}$$

By settig $\alpha = \dfrac{\triangle t}{(\triangle x)^2}$, $\beta = \dfrac{\triangle t}{(\triangle y)^2}$, $\eta = \dfrac{\triangle t}{(\triangle z)^2}$, $\theta = \dfrac{\triangle t}{2\triangle x}$, $\delta = \dfrac{\triangle t}{2\triangle y}$, $\sigma = \dfrac{\triangle t}{2\triangle z}$ and $(u)^m_{i+1,j,k} - (u)^m_{i-1,j,k} = c^m_{i,j,k}$, $G(\xi_x)^m_{i,j,k}$ can be rewritten as:

$$\begin{aligned} G(\xi_x)^m_{i,j,k} = (\beta\nu + \delta v^m_{i,j,k})(\xi_x)^m_{i,j-1,k} + (\alpha\nu + \theta u^m_{i,j,k})(\xi_x)^m_{i-1,j,k} \\ + (\eta\nu + \sigma w^m_{i,j,k})(\xi_x)^m_{i,j,k-1} + [1 + \theta c^m_{i,j,k} - 2\nu(\alpha + \beta + \eta)](\xi_x)^m_{i,j,k} \\ + (\alpha\nu - \theta u^m_{i,j,k})(\xi_x)^m_{i+1,j,k} + (\beta\nu - \delta v^m_{i,j,k})(\xi_x)^m_{i,j+1,k} \\ + (\eta\nu - \sigma w^m_{i,j,k})(\xi_x)^m_{i,j,k+1}. \end{aligned} \tag{40}$$

We note that the summation of all the coefficients on the right-hand side of equation (40) is less than or equal unity if $\theta c^m_{i,j,k} \leq 0$. That is

$$(\beta\nu + \delta v^m_{i,j,k}) + (\alpha\nu + \theta u^m_{i,j,k}) + (\eta\nu + \sigma w^m_{i,j,k}) + [1 + \theta c^m_{i,j,k} - 2\nu(\alpha + \beta + \eta)]$$

$$+(\alpha\nu - \theta u^m_{i,j,k}) + (\beta\nu - \delta v^m_{i,j,k}) + (\eta\nu - \sigma w^m_{i,j,k}) = 1 + \theta c^m_{i,j,k} \leq 1.$$

To ensure that the coefficients are positive, the following conditions must be satisfied:

1. $\mid \theta u^m_{i,j,k} \mid \leq \alpha\nu$. Hence, $\alpha\nu + \theta u^m_{i,j,k} \geq 0$ and $\alpha\nu - \theta u^m_{i,j,k} \geq 0$.
2. $\mid \delta v^m_{i,j,k} \mid \leq \beta\nu$. Hence, $\beta\nu + \delta v^m_{i,j,k} \geq 0$ and $\beta\nu - \delta v^m_{i,j,k} \geq 0$.
3. $\mid \sigma w^m_{i,j,k} \mid \leq \eta\nu$. Hence, $\eta\nu + \sigma w^m_{i,j,k} \geq 0$ and $\eta\nu - \sigma w^m_{i,j,k} \geq 0$.
4. $\mid \theta c^m_{i,j,k} - 2\nu(\alpha + \beta + \eta) \mid \leq 1$. Then, $1 + \theta c^m_{i,j,k} - 2\nu(\alpha + \beta + \eta) \geq 0$.

In addition, we conclude that the summation of the coefficients is positive. Since all the coefficients on the right-hand side of equation (40) are positive and their summation is positive and less than or equal to unity, then the function $G(\xi_x)^m_{i,j,k}$ is bounded as follows:

$$\min \lambda \leq G(\xi_x)^m_{i,j,k} \leq \max \lambda, \quad \text{where}$$

$$\lambda = [(\xi_x)^m_{i,j-1,k}, (\xi_x)^m_{i-1,j,k}, (\xi_x)^m_{i,j,k-1}, (\xi_x)^m_{i,j,k}, (\xi_x)^m_{i+1,j,k}, (\xi_x)^m_{i,j+1,k}, (\xi_x)^m_{i,j,k+1}] .$$

Hence, sufficient, but not necessary, stability conditions for equation (37) are given by:

$$\theta c^m_{i,j,k} \leq 0, \ \mid u^m_{i,j,k} \mid \leq \frac{2\nu}{\triangle x}, \ \mid v^m_{i,j,k} \mid \leq \frac{2\nu}{\triangle y}, \ \mid w^m_{i,j,k} \mid \leq \frac{2\nu}{\triangle z}, \ \text{ and}$$

$$2\nu(\alpha + \beta + \eta) \leq 1 + \theta c^m_{i,j,k}.$$

The last condition is equivalent to

$$2\nu(\alpha + \beta + \eta) \leq 1 .$$

Thus, the stability requirement for this method is

$$(\triangle t) \leq \frac{Re}{2\left[\frac{1}{(\triangle x)^2} + \frac{1}{(\triangle y)^2} + \frac{1}{(\triangle z)^2}\right]}, \tag{41}$$

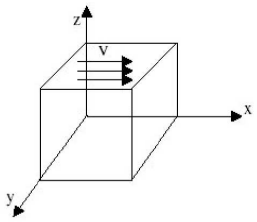

Figure 1: The lid-driven cavity in 3D

where $Re = \dfrac{1}{\nu}$ is the Reynolds number.

A Time-Marching Algorithm. The following algorithm provides an outline of the code, which we implemented. The presented disrcetization schemes, numerical techniques, boundary conditions, and stability conditions were taken into consideration during the numerical implementation. In summary, the process is implemented as follows:

1. Initialize the values of ξ and ψ.
2. Solve for ξ using the vorticity transport equation.
3. Solve for ψ using the Poisson equation.
4. Update the velocity, by substituting the resulting values of ψ in the finite-difference formulation of equation (11). For example, we obtain the component u of the velocity $V = (u, v, w)$ as follows:

$$u^m_{i,j,k} = \frac{(\psi_z)^m_{i,j+1,k} - (\psi_z)^m_{i,j-1,k}}{2\triangle y} - \frac{(\psi_y)^m_{i,j,k+1} - (\psi_y)^m_{i,j,k-1}}{2\triangle z}.$$

5. Determine values of ξ and ψ on the boundaries.
6. Repeat steps 2 through 5 until the solution converges.

5. Results and Analysis

Numerical results for Poisson equation have been presented in a previous publication [1]. This section presents the results of studying the model problem of the lid-driven laminar flow in a 3D cubic cavity ($1 \times 1 \times 1$). The geometry of

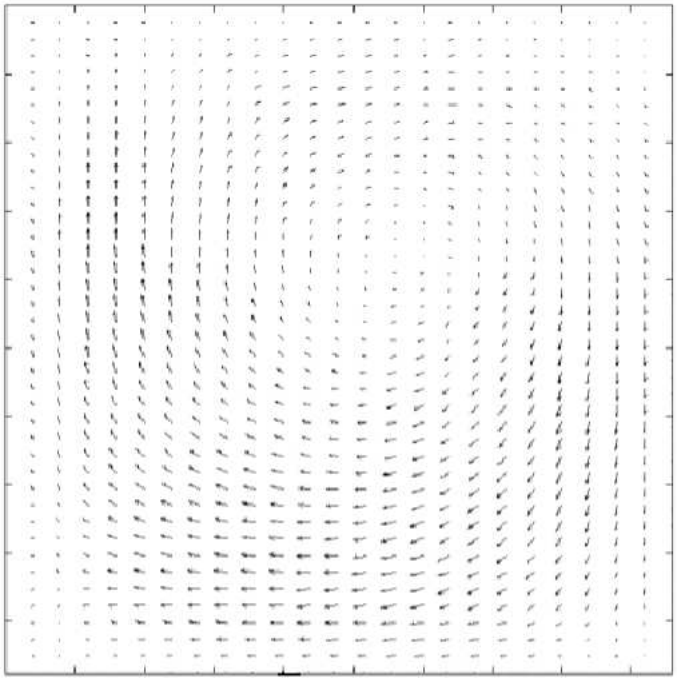

Figure 2: Flow direction vectors on $y = 0.5$ ($Re = 400$)

the cubic cavity is shown in Figure 1. The velocities vanish everywhere at the boundary except at the upper boundary.

The solution procedure starts by solving the vorticity transport equation based on the initial values. Then, we solve the Poisson equation. The iterative computation for Poisson equation continues until a relative convergence criterion of 10^{-5} is achieved. Finally, the new velocities are evaluated. This procedure is repeated until a velocity field with an absolute convergence criterion of 10^{-5} is reached. As a result of a series of mesh convergence tests using various mesh systems, we used a mesh of 25 (x-direction) $\times$ 25 (y-direction) $\times$ 41 (z-direction) for $Re = 400$ and 31 (x-direction) $\times$ 31 (y-direction) $\times$ 47 (z-direction) for $Re = 1000$. Figures 2-4 display the velocity vector plots on the three mid-planes $x,\ y,\ z = 0.5$ for $Re = 400$ and Figures 5-7 display the velocity vector plots for $Re = 1000$ on the three mid-planes $x,\ y,\ z = 0.5$. These velocity profiles are in good agreement with other published results [11, 12, 20].

The velocity vector plots at the midplanes $x = 0.5$ and $z = 0.5$, shown in

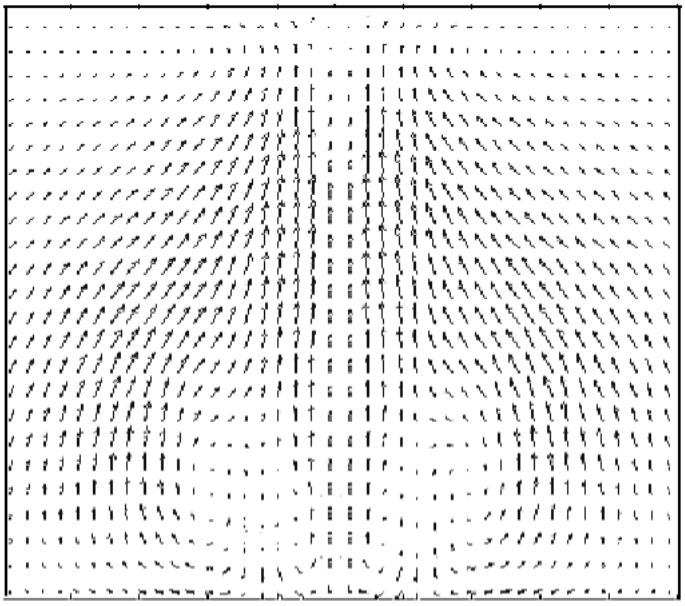

Figure 3: Flow direction vectors on $x = 0.5$ ($Re = 400$)

Figure 3 and Figure 4 respectively, clearly illustrate the onset of contra-rotating transversal vortices, which strengthen with increasing Reynolds numbers and became more distinctive at $Re = 1000$ as displayed in Figure 6 and Figure 7. Moreover, the pair of primary vortices on the plane $x = 0.5$ is seen to shift towards the lower corners of the cavity as the Re is increased from 400 to 1000. Meanwhile, a pair of secondary vortices near the upper corners becomes increasingly discernible, as concluded from Figure 3 and Figure 6. This has also been observed in previous studies [12].

It should be pointed out that for higher Re, there are nonlinear variations in the velocity in a small region near the boundary as inferred from Figure 3 and Figure 6. Since we are using a uniform grid, we need higher discretization for higher Re numbers. In addition, the symmetry of the velocity field with respect to the midplane $y = 0.5$ can be detected from Figure 8.

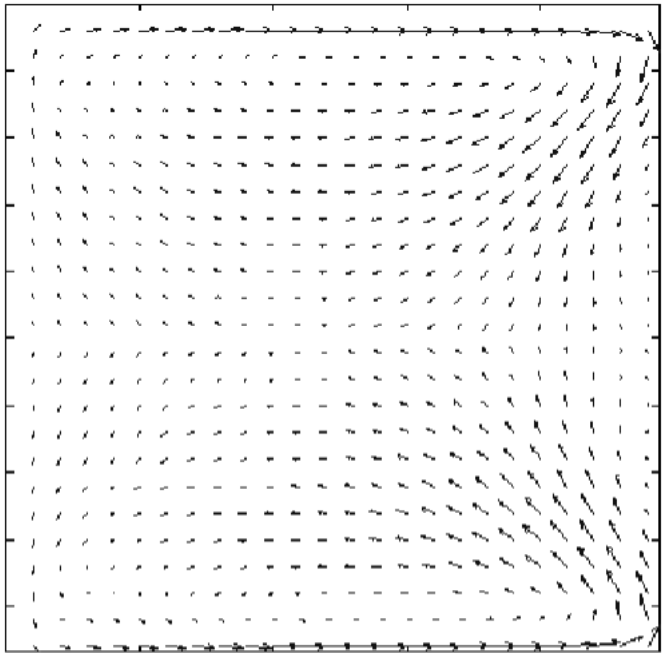

Figure 4: Flow direction vectors on $z = 0.5$ ($Re = 400$)

6. Conclusions and Future Work

In this paper, we have presented a numerical approach for solving incompressible Navier-Stokes equations in 3D by finite difference techniques. Compared to previously published results, the numerical results obtained are of high quality [4, 11, 12, 14, 15, 18, 24]. In summary, the advantages of our approach are:

1. The pressure need not be calculated explicitly in vorticity-vector potential approach. Hence, the boundary conditions are easier to apply.

2. The Poisson equation is solved using an iterative technique to eliminate the limitation on grid size. For the same reason, Euler explicit method is used for the vorticity transport equation.

3. A necessary stability condition is derived for the vorticity transport equation.

4. A time-marching algorithm is implemented for facilitating the computation of the velocities.

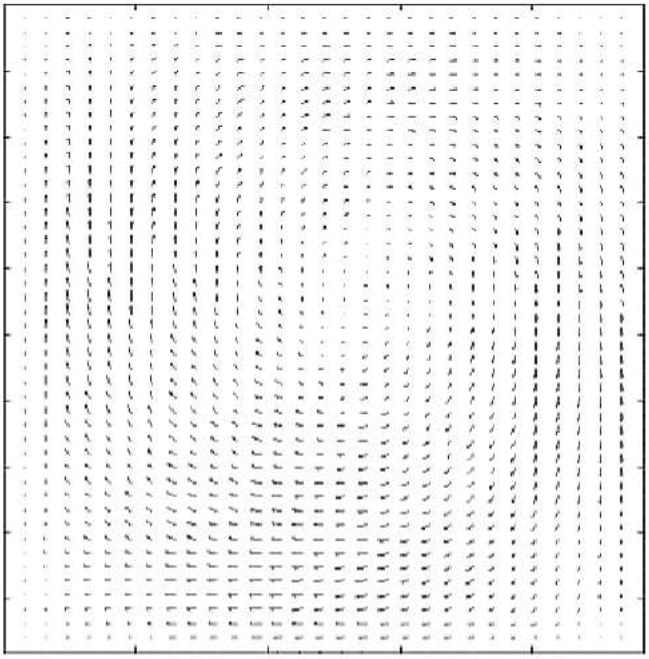

Figure 5: Flow direction vectors on $y = 0.5$ ($Re = 1000$)

Finally, we envision some aspects, which can be considered in future work:

1. High order schemes can be used to increase the accuracy in some computations. The derivatives used in Poisson equation, in the boundary conditions and in calculating the velocities are candidates for such improvements.

2. Sufficient and necessary conditions for stability can be deduced, rather than the sufficient conditions that we have deduced.

3. Generalizations of the presented methods to other geometries, grids and model problems can be preformed.

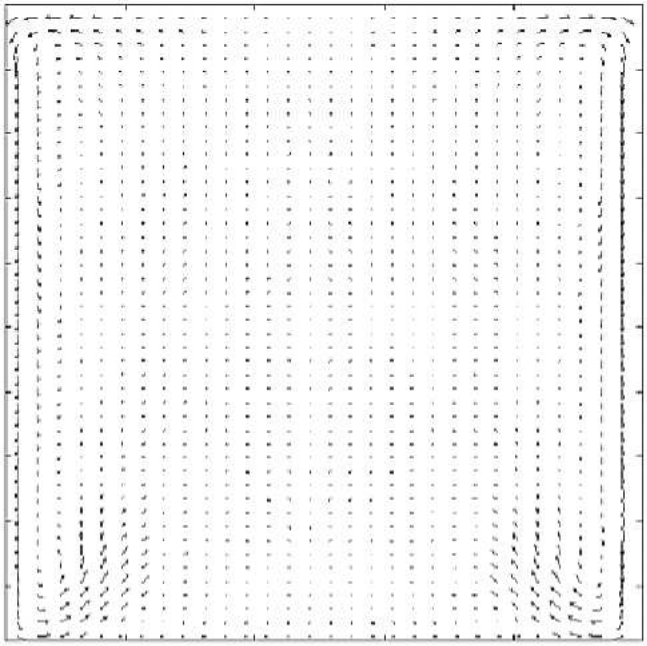

Figure 6: Flow direction vectors on $x = 0.5$ ($Re = 1000$)

References

[1] S.K. Abd-El-Hafiz, G.A.F. Ismail, B.S. Matit, A numerical technique for the 3-D Poisson equation, *Int. J. of Pure and Applied Mathematics*, **7** (2003), 263-270.

[2] D. Anderson, J. Tannehill, R. Pletcher, *Computational Fluid Mechanics and Heat Transfer*, McGraw-Hill, New York (1994).

[3] K. Aziz, J.D. Hellums, Numerical solution of the three-dimensional equations of motion for laminar natural convection, *The Physics of Fluids*, **10** (1967), 314-324.

[4] D. Choi, C.L. Merkle, Application of time-iterative schemes to incompressible flow, *AIAA-Journal*, **23** (1985), 1518-1524.

[5] J. Chorin, The numerical solution of the Navier-Stokes equations, *Mathematics and Computing*, **22** (1968), 745-762.

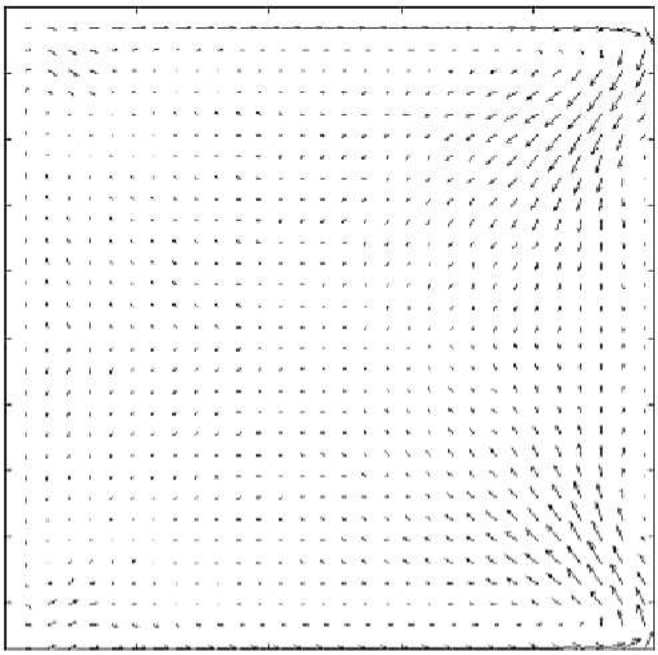

Figure 7: Flow direction vectors on $z = 0.5$ ($Re = 1000$)

[6] J. Chorin, *Computational Fluid Mechanics: Selected Papers*, Academic Press (1989).

[7] M.J. Crochet, A.R. Davies, K. Walters, *Numerical Simulation of Non-Newtonion Flow*, Elsevier, New York (1984).

[8] W. Dai, R. Nassar, A compact finite difference scheme for solving three dimensional heat transport equation in a thin film, *Numerical Methods for Partial Differential Equations*, **16** (2000), 441-458.

[9] L. Ge, J. Zhang, Accuracy, robustness, and efficiency comparison in iterative computation of convection diffusion equation with boundary layers, *Numerical Methods for Partial Differential Equations*, **16** (2000), 379-394.

[10] L. Ge, J. Zhang, High accuracy iterative solution of convection diffusion equation with boundary layers on non-uniform grids, *J. of Computational Physics*, **171** (2001), 560-578.

[11] G. Guj, F. Stella, A vorticity-velocity method for the numerical solutions

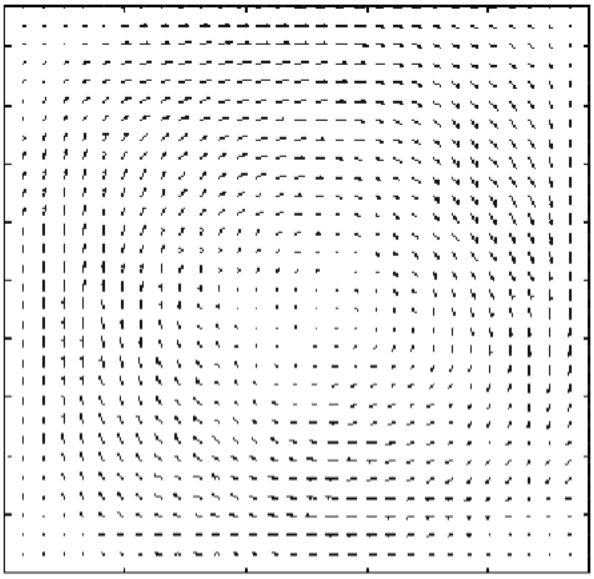

Figure 8 (a): Flow direction vectors for ($Re = 1000$) on $y = 0.043$

of 3-D incompressible flows, *J. of Computational Physics*, **106** (1993), 286-298.

[12] C.J. Ho, F. H. Lin, Numerical simulation of three-dimensional incompressible flow by a new formulation, *Int. J. of Numerical Methods in fluids*, **23** (1996), 1073-1084.

[13] K.W. Morton, M. J. Baines, *Numerical Methods for Fluid Dynamics*, Clarendon Press, Oxford (1986).

[14] M. Napolitano, G. Pascazio, L. Quartapelle, A review of vorticity conditions in the numerical solution of the [vorticity and stream function] equations, *Computers and Fluids*, **28** (1999), 139-185.

[15] S.V. Patanker, *Numerical Heat Transfer and Fluid Flow*, Hemishpere Publishing Co. (1980).

[16] S.V. Patanker, D.B. Spalding, A calculation procedure for heat, mass and momentum transfer in three-dimensional parabolic flows, *Int. J. of Heat Mass Transfer*, **15** (1972), 1787-1806.

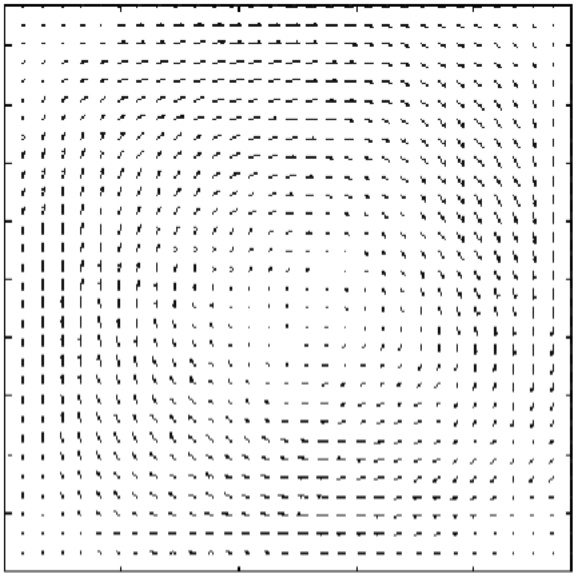

(b)

Figure 8 (b): Flow direction vectors for ($Re = 1000$) on $y = 0.957$

[17] A. Pujol, *Numerical Experiments on the Stability of Poiseuille Flows of Non-Newtonian Fluids*, Ph.D. Dissertation, University of Iowa, Iowa City, Iowa, (1971).

[18] P.J. Roache, *Fundamentals of Computational Fluid Dynamics*, Hermosa Publisher (1998).

[19] W.F. Spotz, Accuracy and performance of numerical wall boundary conditions for steady, 2D, incompressible stream function vorticity, *Int. J. for Numerical Methods in Fluids*, **28** (1998), 737-757.

[20] S. Turek, *Efficient Solvers for Incompressible Flow Problems: An Algorithmic and Computational Approach*, Springer-Verlag (1999).

[21] E. Weinan, Numerical methods for viscous incompressible flow: some recent advances, *J. of Computational Physics*, **124** (1996), 181-195.

[22] E. Weinan, J.G. Liu, Vorticity boundary condition and related issues for finite difference schemes, *J. of Computational Physics*, **124** (1996), 368-382.

[23] P. Wesseling, *Principles of Computational Fluid Dynamics*, Springer-Verlag, Berlin (2000).

[24] P. Wesseling, A. Segal, C.G.M. Kassels, Computing flows on general three-dimensional non-smooth staggered grids, *J. of Computational Physics*, **149** (1999), 333-362.